LIMITATIONS OF THE GROWTH RATE OF SILICON MONO INGOTS GROWN BY THE CZOCHRALSKI TECHNIQUE

F. Mosel[1], A.V. Denisov[1], B. Klipp[1], N. Sennova[1], C. Kranert[2,3], T. Jung[3], M. Trempa[3], C. Reimann[2,3], J. Friedrich[2,3]
[1] PVA Crystal Growing Sytems GmbH, Im Westpark 10-12, 35435 Wettenberg, Germany
[2]Fraunhofer Technologiezentrum Halbleitermaterialien THM, Am St.-Niclas-Schacht 13, 09599 Freiberg, Germany
[3]Fraunhofer-Institut für Integrierte Systeme IISB, Schottkystraße 10, 91058 Erlangen, Germany
e-mail: frank.mosel@pvatepla.com
tel: +49 64168690-125, fax: +49 64168690-822

ABSTRACT In the PV industry, cost pressure subsists in the entire production chain of PV modules, affecting the further development of high-performance cell concepts and the manufacture of suitable high quality substrate crystals. The improvement of the quality of monocrystalline silicon ingots, grown by the Czochralski technique, while increasing productivity and reducing crystallization costs, is a major challenge. The reductions in production costs can be achieved by increasing growth rate and melt volumes. Both options were shown at EUPVSEC 2016 [1]. In this contribution we have investigated the basic limitations of the pull rate in the Czochralski process. As part of our investigations we have grown several crystals beyond the pulling speed limit resulting in a loss of the cylindrical shape of the ingot, often described as twisting or spiral growth. We performed these crystal growth experiments in various crystal growing configurations using different process parameters. We have analyzed the boundary conditions by means of numerical simulation calculations and compared the results with the crystal growth experiments. From this, we have derived diagrams that allow an estimation of the pull rate limit for the different growth conditions. We have found a simple relationship between the growth rate and the deflection of the phase boundary allowing the growth conditions to be assessed in terms of the stability criteria mentioned above. We show that by the application of an active crystal cooler during the growth process in combination with a suitable inner heat shield the deflection of the growth interface can be influenced. This fact can be used to realize a higher pull speed and to influence the material quality of the growing crystal.

Keywords: c-Si, active crystal cooling, growth rate, spiral growth, twisting

1 INTRODUCTION

In order to reduce the manufacturing costs of monocrystalline dislocation-free silicon crystals applying the Cz-technique, two main routes are followed. The melt quantities used per process cycle are increasing. In addition to larger crucible dimensions (initial loads), this also includes the application of the multipulling technique [1]. Furthermore, the production rate must be increased. In addition to an optimization of the process flow, this primarily includes an increase of the pull speed during the Czochralski process. However, there are physical limits to a stable cylindrical growth of the silicon ingot. The heat transport from the melt and the released heat of crystallization must be dissipated fast enough through the growing crystal. The heat of crystallization increases with increasing pull speed, which in turn leads to an increase of the concave deflection of the crystal-melt interface and a reduction of the radial temperature gradient at the melt meniscus. As a fact supercooled areas near the phase boundary may occur leading to a loss of the cylindrical shape of the growing crystal [2]. Using numerical simulation tools, we analyzed the influence of the phase boundary shape and the radial temperature distribution on the melt surface and the stability of crystal growth. We have found a direct relation between the deflection of the concave interface deflection and the occurrence of the loss of the cylindrical shape of the growing crystal. We have developed stability diagrams for different crystal growth conditions. These stability diagrams were confirmed by crystal growth experiments. For this purpose, the curvature of the phase boundaries (interface deflection) of the crystals were examined with LPS[1] measurements and compared with the results of the numerical simulations. We show that stable growth conditions for an increased pull speed on the one hand and for a small deflection of the interface on the other hand can be found out applying these diagrams.

2 EXPERIMENTAL

2.1 Limitation of the growth rate in Cz-configuration

The physical rate limiting parameter for the growth of ingots in a Czochralski configuration is the dissipation of the latent heat of fusion of silicon at the interface crystal/melt by heat conduction through the growing ingot. The heat received from a crystal in contact with the melt can be determined as the heat of solidification plus the heat flux from the melt into the ingot. This situation can be written in a simple one dimensional model [3]:

$$\lambda_s \cdot \mathrm{A} \cdot \left(\frac{dT}{dx}\right)_S = \lambda_l \cdot \mathrm{A} \cdot \left(\frac{dT}{dx}\right)_l + \rho \cdot \mathrm{A} \cdot L \cdot v_p \qquad \text{(I)}$$

In which λ is the thermal conductivity, A the area of the interface, (dT/dx) is the axial temperature gradient, v_p is the constant growth velocity, ρ is the crystal density, L the latent heat of fusion and s,l are the subscripts for the solid and liquid phase. The heat of crystallization is directly correlated to the growth rate, which is shown in tab.1.

[1] Lateral photovoltage scanning [4]

growth rate [mm/min]	latent heat [kW]
0.9	2.3
1.8	4.6

Table I: Released heat of crystallization for 8 inch ingots

2.2 Crystal growth

The crystal growth experiments presented in this paper were performed in different crystal growth configurations applied in a SC22 and SC24/26 Czochralski-puller from PVA Crystal Growing Systems GmbH (see fig.1). The most important parameters of the different hot zones are given in tab.II. All crystals grown in the reported experiments had a diameter of 8 inches. The different crystal growth configurations were investigated theoretically and experimentally in order to evaluate the main key parameters influencing the growth rate limit.

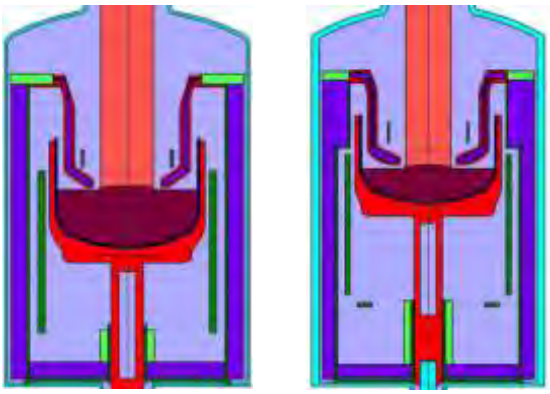

Figure 1: Crystal growth configuration of V1 (left) and V2, V3 (right).

growth configuration	crucible dimension [inch]	bottom heater	ACC
Va	22/24	no	no
V1	22	no	yes
V2basic	24	no	no
V2	24	yes	yes
V3	26	yes	yes

Table II: Crystal growth configurations

Some of the crystals grown in the different growth configurations were prepared for characterization according to fig.13 and fig.19. The vertically cut samples have been examined at Fraunhofer THM using LPS measurements. The measured deflections of the phase boundary H (fig.2), which were determined at a body length of 500 mm, are summarized in tab.III. In the case of the twisted crystals, the transition area from stable to unstable growth was directly examined.

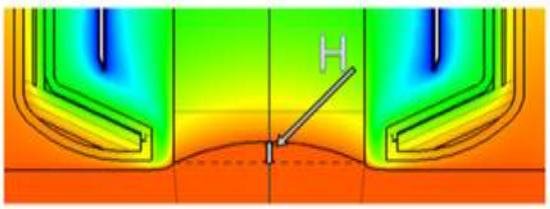

Figure 2: Sketch of the cooling device and the inner heat shield. H indicates the deflection of the phase boundary.

mean pull speed in body phase [mm/min]	mean pull speed at twisting onset [mm/min]	body length at twisting onset [mm]	deflection exp. at 500 mm	deflection calc. at 500 mm	twisting
-	1.1	620	25	24	yes
-	1.1	600	18	14	yes
1.2			3	6	no
-	1.1	500	-	24	yes
0.9			13	13	no
1.3			21	23	no
1.8			21	21	no
1.6			13	13	no

Table III: Relationship between growth rate and interface defection.

2.3 Transition from stable to unstable (twisted) growth

During the growth of [100]-oriented dislocation-free silicon crystals, four growth ridges appear parallel to the growth axis and perpendicular to the in-plane <011>-directions. The shape of the growth ridges depends on the temperature field and the melt meniscus [5].The stability of the crystal growth process can be assessed on the basis of the appearance of the growth ridges. Stable growth is characterized by narrow parallel trailing edges as outlined in fig.3 (left).

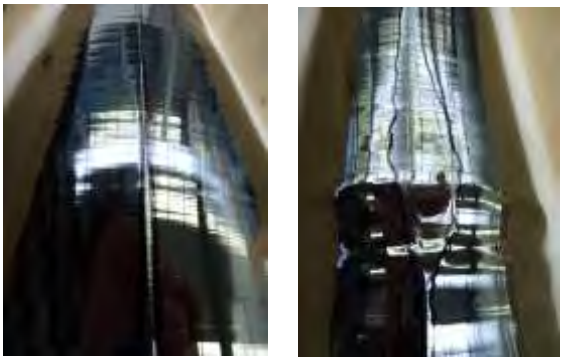

Figure 3: Appearance of the growth ridges (framed in black).

Temperature instabilities on the melt meniscus cause an irregular development of the growth ridges. In our crystal growing experiments, we observed a clear asymmetry and broadening of the growth ridges before the onset of twisting, which is shown in fig.3 (right). The asymmetry and widening of the growth ridge can be clearly seen, which indicates the loss of the cylindrical symmetry even in a very early stage of crystal growth.

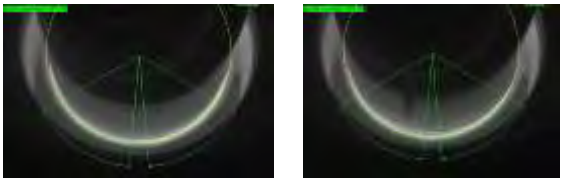

Figure 4: Snapshot of the process camera showing stable (left) and unstable (right) growth conditions.

Fig.4 (left) shows a snapshot of the process camera during stable growth conditions and at the onset of spiral growth (right). In the latter case an asymmetrical formation of the crescent shaped meniscus (bright ring) can be seen, which is also apparent in the data recording of the diameter, shown in fig.5. The graphic shows the fluctuation of the center of the circle which is interpolated onto the growing crystal. A slight basic

vibration can be seen, which corresponds to a slight pendulum movement of about 0.5 mm of the crystal hanging on its cable. The gradual onset of twisting is indicated by an increasing fluctuation of the recorded circle center. Fig. 6 shows the corresponding recorded diameter reflecting the maximum of the spiral growth (twisting) at 900 mm of the total length (from neck to tail).

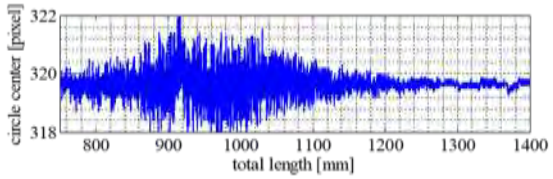

Figure 5: Horizontal vibration of the center of the interpolated circle.

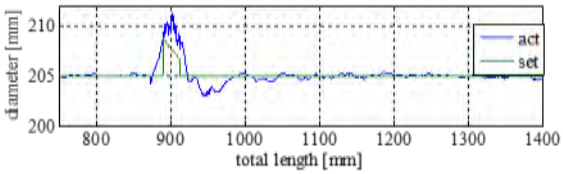

Figure 6: Recorded diameter of the process camera.

Both the temporal formation of the growth ridges and the camera signal enable early detection of an indicated loss of the cylindrical symmetry.

2.4 Investigation of the different crystal growth configurations

We examined the influence of the growth parameters on the crystal growth by means of numerical simulation calculations using the commercially available CGSim-software package from STR Group[2]. The variant for 2D simulation was applied to keep the time required for the calculations low. Different crystal growth configurations were examined, the main features of which are listed in tab II. The essential criteria for the assessment are the deflection of the phase boundary in the crystal center (interface deflection H) and the temperature distribution n the area of the melt meniscus of the growing crystal [2]. The curvature of the interface should be as plane as possible and the axial temperature gradient at the triple point should be steep for stable growth conditions. The results of the simulation calculations were evaluated at a body length of 500 mm of the growing ingot. Fig.7 shows the interface curvature H of the phase boundary versus the average pull speed for different growth configurations. The symbols in the figure represent individual results of the simulations. A linear relationship between the average pull speed and the deflection of the phase boundary is evident and indicated by the inserted lines. The figure represents a stability diagram in which three areas are marked. In the stable growth region (green) the system is insensitive to changes in the average pull speed. This region is robust and suitable for industrial production. In the metastable growth region (yellow) all growth parameters have to be well tuned. Small changes can lead to unstable growth with loss of the cylindrical shape, i.e. spiral growth. In the unstable growth region (red) no regular crystal growth is possible.

[2]STR Group, Inc., St. Petersburg, Russia

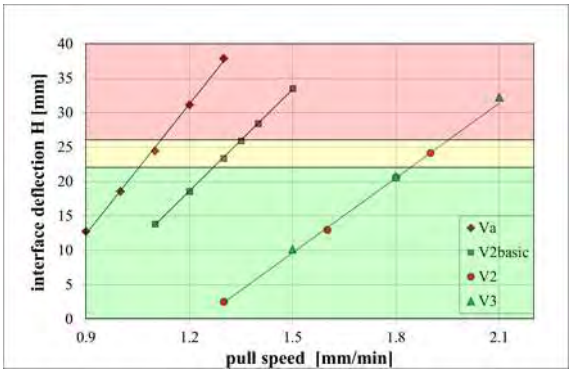

Figure 7: Stability diagram for different crystal growth configurations**.**

The differences of the various crystal growth configurations can be mainly assigned to the optimized geometry of the inner heat shield in combination with an active crystal cooling device (V2 and V3). The configurations V2 and V3 differ only in the enlargement of the crucible diameter from 24 to 26 inches, which obviously has no influence on the phase boundary shape in the applied growth configurations. The diagram also shows the basic setup of the 22 and 24 hotzone (Va) without crystal cooler. Its influence on the interface deflection is obvious. $V2_{basic}$ shows the optimized hotzone design of Va, also without active crystal cooler. The graphic clearly shows the influence of the active crystal cooling on the interface deflection and thus on the average pull speed, which should be applicable in the examined crystal growth configuration.

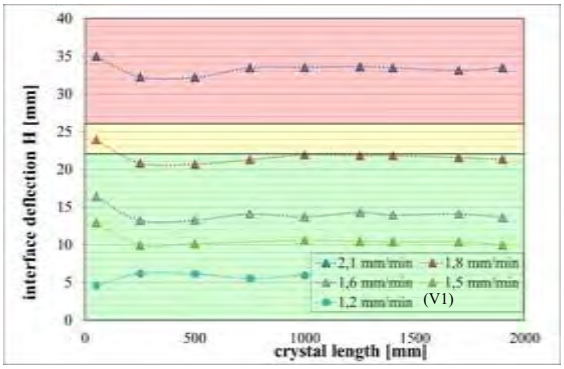

Figure 8: Variation of the interface deflection for different growth rates applied in the body phase in crystal growth configuration V1 for the growth rate of 1.2 mm/min and V2/V3 for the other growth rates.

Fig.8 shows the variation of the interface deflection over the body length calculated for the configuration V2/V3 with active crystal cooling and different growth rates. From a length of about 300 mm, the phase boundary shows an approximately constant deflection which is confirmed by the LPS-measurements (see fig.18 - fig.23). In addition, a result from the configuration V1 is also shown in order to illustrate the effect of crystal cooling on the interface deflection. The curves of V3 with 1.6 mm/min and V1 with 1.2 mm/min were confirmed over the entire crystal length by real crystal growth experiments (chap. 3).

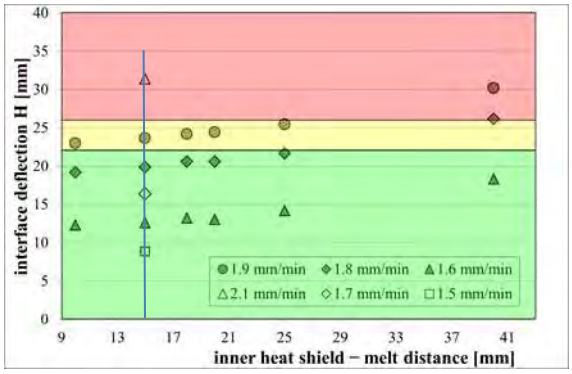

Figure 9: Interface deflection for different melt gaps applied with different growth rates in crystal growth configuration V2/V3.

Fig.9 shows the influence of the gap between the lower edge of the inner heat shield and the melt surface for different average growth rates applied in the crystal growth configuration V2/V3. The straight line indicates the applied gap of the crystal shown in fig.17.

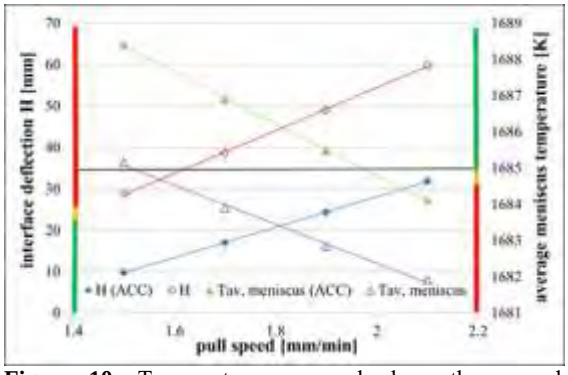

Figure 10: Temperature averaged along the curved meniscus surface and interface deflection versus the average pull speed in crystal growth configuration V2/V3 with (ACC) and without active crystal cooling.

In order to investigate the influence of the growth rate with and without active crystal cooling on the radial temperature distribution near the interface we have calculated the arithmetic mean of the temperature on the curved meniscus surface (2-d simulations). In fig.10 the average meniscus temperature and the interface deflection are plotted versus the mean pull speed. The diagram suggests that areas of thermally supercooled melt can occur as the growth rate increases, which is confirmed by the work of Friedrich et al. [2]. Trends in the graphic that should be avoided for stable growth conditions are marked by the colored side bars.

3 RESULTS

3.1 Characterization of the crystals

According to fig.13 and fig.19 vertically cut slices from the different crystals (tab.IV) have been prepared for LPS measurements. An example of this characterization technique is shown in fig.11. Based on the LPS images, the phase boundary shapes were reconstructed and axial distributions of the interface deflection H were determined.

ingot	mean pull speed in body phase [mm/min]	mean pull speed at twisting onset [mm/min]	body length at twisting onset [mm]	deflection exp. at 500 mm	deflection calc. at 500 mm	twisting
A	1.1 - 0.9	1.1	620	25	24	yes
B	1.1 - 0.75	1.1	600	18	14	yes
C	1.2	-	-	3	6	no
D	1.6	-	-	13	13	no

Table IV: Summary of the characterized ingots

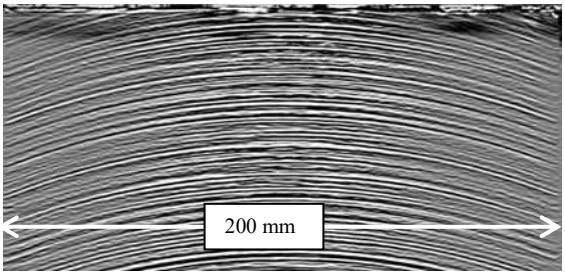

Figure 11: Growth striations revealed by the LPS technique on a vertically sliced sample indicating the deflection of the growth interface.

3.1.1 Twisted Crystals

Fig.11 shows the ingot A (see tab.IV) which reveals a twisted part of its body.

Figure 12: Crystal with a deviation from the cylindrical shape (spiral growth).

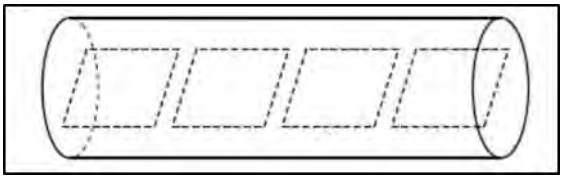

Figure 13: Sketch of the prepared samples.

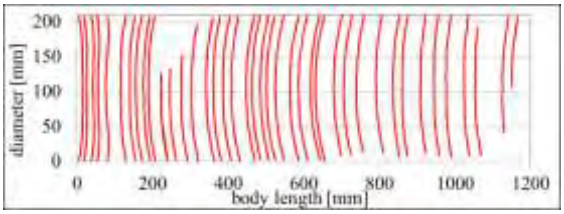

Figure 14: Distribution of the phase boundary in the body of ingot A.

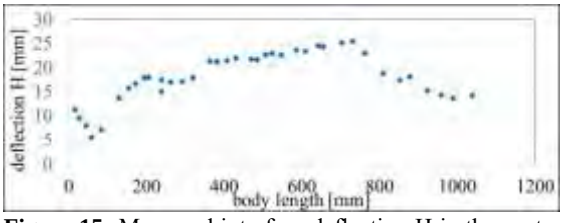

Figure 15: Measured interface deflection H in the center of the ingot A.

The characterization results of a crystal (ingot B) with a weaker formation of spiral growth is shown in fig.16 – fig.17.

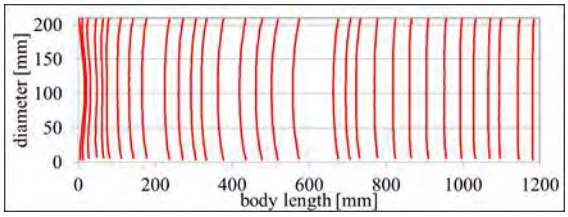

Figure 16: Distribution of the phase boundary in ingot B.

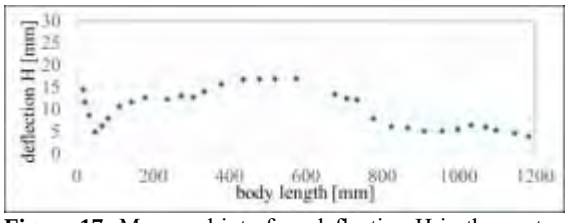

Figure 17: Measured interface deflection H in the center of the ingot B.

We have also examined two crystals in the same way as described above which were grown under stable growth conditions.

3.1.2 Regular shaped crystals

We have grown two crystals under stable conditions and also examined the axial development of the phase boundary. One of the crystals was produced with an increased pull speed (ingot D). The pull speed of the other crystal was reduced with the aim of an almost flat phase boundary (ingot C). The results of the characterizations are shown in the following figures.

Figure 18: Crystal with a regular cylindrical shape.

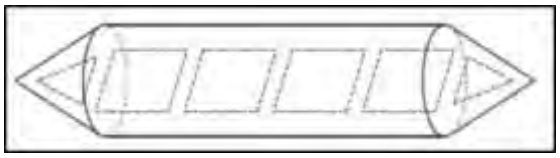

Figure 19: Sketch of the prepared samples.

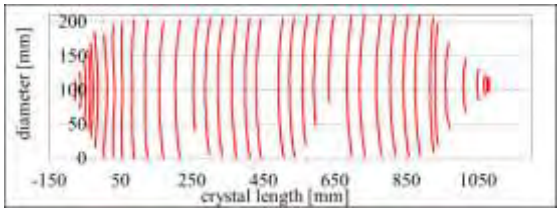

Figure 20: Distribution of the phase boundary in the whole ingot D.

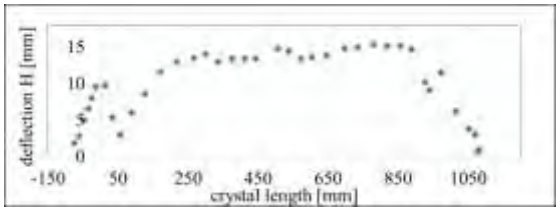

Figure 21: Measured interface deflection H in the center of the ingot D.

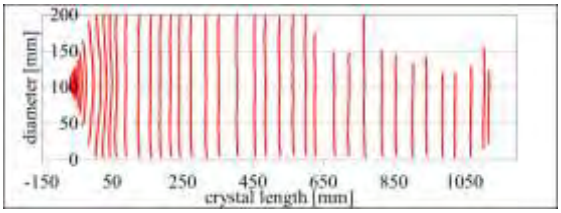

Figure 22: Distribution of the phase boundary in the whole ingot C.

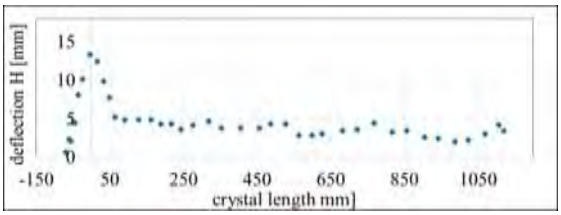

Figure 23: Measured interface deflection H in the center of the ingot C.

We have proven the calculated stability diagrams (fig.7-fig.9) by several crystal growth experiments. We noticed the onset of twisting and compared it with our calculations. In the growth experiments of ingot A and ingot B, the growth conditions have been changed during the twisted growth in order to return to regular cylindrical growth. The pull speed and the crucible rotation were reduced. These measures for example enabled cylindrical growth to be restored after a certain time. In the LPS profiles, the transition from irregular to regular growth is accompanied by a decrease of the interface deflection. By reducing the growth rate, the heat of crystallization is reduced, which in turn leads to a reduction in the deflection.

The use of active crystal cooling increases the effective radiation exchange between the growing crystal and its surroundings, which leads to a steeper temperature gradient at the phase boundary (I) allowing a higher growth rate. Active crystal cooling can also be used to ensure stable crystal growth conditions or to reduce the interface deflection. Fig. 20 shows the result of a crystal that was pulled with an increased pulling speed and a moderate deflection of the phase boundary. Fig.23 shows a crystal, which was grown with a nearly flat interface. Both results demonstrate the potential of an active crystal cooling in the Czochralski process.

4 DISCUSSION

A high pull speed is often cited as the cause of structural loss due to the generation of dislocations as a result of an increased interface deflection enhancing thermal stresses at the interface [6]. We have calculated the von-Mises stresses for the different crystal growth configurations (tab.V) and compared the results with experimentally determined values which have been measured by means of Scanning Infrared Stress Depolarization [7], an example is shown in fig. 24.

growth configuration	mean pull speed in body phase [mm/min]	deflection calc. at 500 mm	twisting	von-Mises stress [Pa]
Va	1.1 - 0.9	24	yes	3.90E+07
V1	1.1 - 0.75	13.5	yes	2.70E+07
V1	1.2	6	no	2.90E+07
Va	1.1 - 0.85	24	yes	3.90E+07
Va	0.9	13	no	3.00E+07
V2basic	1.3	23	no	4.60E+07
V2	1.8	21	no	6.20E+07
V3	1.6	13	no	4.10E+07

Table V: Maximum calculated von-Mises stresses for the different crystal growth conditions.

For this characterization technique we have applied the SIRD system from PVA Metrology & Plasma Solutions GmbH. No differences between the examined samples were observed. All samples are stress-free exept the outer edge area. Along the circumference, the samples show slight tensile stresses, which may indicate a certain defect structure.

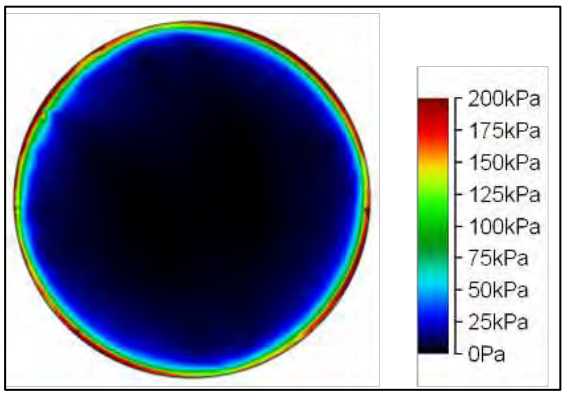

Figure 24: Shear stress maximum in the sample cut from the middle of a crystal grown in configuration V2/V3.

Based on the results of tab.V, it is assumed that the interface deflection alone does not correlate with the calculated von-Mises stresses. There is also no correlation with spiral growth. We also conclude that the interface deflection in combination with the enhanced latent heat due to the pull speed is the cause of the occurrence of spiral growth.
From our point of view the amplitude and frequency of temperature fluctuations may be crucial for dislocation formation. Friedrich et al. [2] have calculated the temperature fluctuations at the free melt surface for different pull speeds, shown in fig.25 (reproduced from [2]). Local and temporal remelting seem to occur at high growth rates resulting in an increasing probability of dislocation formation. These temperature fluctuations should be avoided in any case for a dislocation free crystal growth.
This item will be a topic for our following research work.

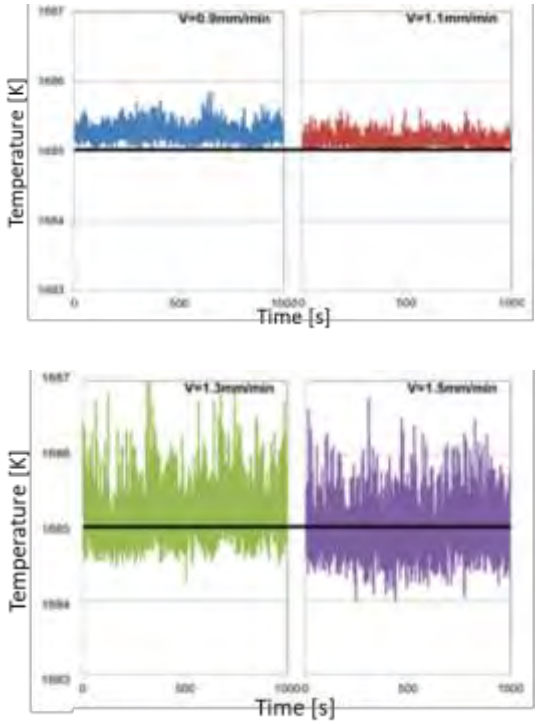

Figure 25: Temperature fluctuations at the free melt surface close to the triple point in a coordinate system rotating with the crystal for different pull rates 0.9mm/min, 1.1mm/min, 1.3mm/min, and 1.5mm/min. The calculations were performed for 26" crucible, 190kg initial charge weight, 100cm crystal length, and no active crystal cooler

This work was supported by the German Federal Ministry for Economy Affairs and Energy under contract number 0324281B and 0324357B

7 REFERENCES

[1] F. Mosel, A.V. Denisov, B. Klipp, N. Sennova, M. Herms, R. Kunert, P. Dold, Proceedings 35th European Photovoltaic Solar Energy Conference, Brussels, Belgium, (2018) 476-482
[2] J. Friedrich, T. Jung, M. Trempa, C. Reimann, A.V. Denisov, A. Mühe, Journal of Crystal Growth **524** (2019) 125168
[3] J.C. Brice, Journal of Crystal Growth **2** (1968) 395-401
[4] N.V. Abrosimov, A. Lüdge, H.Riemann, W. Schröder, Journal of Crystal Growth **237-239** (2002) 356-360
[5] L. Stockmeier, C. Kranert, P. Fischer, B. Eppelbaum, C. Reimann, J. Friedrich, G. Raming, A. Miller, Journal of Crystal Growth **515** (2019) 26-31
[6] O.V. Smirnova, N.V. Durnev, K.E. Shandrakova, E.L. Mizitov, V.D. Soklakov, Journal of Crystal Growth **310** (2008) 2185-2191
[7] M. Herms, M. Wagner, Phys. Status Solidi C**12**, No.8 (2015) 1085-1089